# Intercummulus massive Ni-Cu-Co and PGE-bearing sulphides in pyroxenite: a new mineralization type in the layered gabbroic sequence of the Beja Igneous Complex (Portugal)

**Ana P. Jesus, António Mateus, José Munhá, Álvaro Pinto**
*CREMINER/Centro Geologia/Dep. Geologia, U. Lisboa, Ed. C6, Campo Grande, 1749-016,Lisboa, Portugal*

**Abstract.** Coarse-grained pyroxenite cumulates occurring within an olivine leucogabbro/pyroxenite gabbro rhythmic suite host a new sulphide mineralization type in the Beja Layered Gabbroic Sequence, Portugal. The sulphides formed in an intercummulus phase as a result of the coalescence of disseminated blebs of pyrrhotite with abundant pentlandite and chalcopyrite exsolutions, gradually disrupting the silicate matrix. Intra- and inter-granular veinlets are sealed by Ni-rich minerals of the linnaeite group, with decreasing Co content from earlier to later generations. The deposition of Ni (± Co)-rich pyrite represents the late mineral infill in the linnaeite veins. Pyrite veinlets and subhedral grains in the pyrrhotite groundmass display gradually lower Ni contents with time. Chalcopyrite is the latest sulphide phase, sealing micro-fractures and replacing pre-existing sulphides. EPMA data revealed concentrations up to 1500 ppm of Pt, Pd, Au, Ag Cd and Bi in pentlandite, chalcopyrite and in minerals of the linnaeite group.

**Keywords.** Layered gabbros, pyroxenite, intercummulus, massive sulphides

## 1 Introduction

The Beja Igneous Complex is an intrusive belt that can be followed for *ca.* 100 km along the southwestern border of the Ossa Morena Zone in Portugal (Fig. 1). The Beja Igneous Complex records syn-orogenic Variscan magmatic activity, extending from Upper Devonian to Late Visean (Dallmeyer et al. 1993). Three units are classically defined within the Beja Igneous Complex: 1) the Beja Layered Gabbroic Sequence (LGS), mainly consisting of olivine-bearing gabbroic rocks, rimmed by heterogeneous diorites resulting from variable extents of magma mixing and crustal assimilation; 2) the Cuba-Alvito Complex comprising granodioritic and gabbroic rocks; and 3) the Baleizão Porphyry Complex, a late, shallow intrusion consisting of porphyritic granitoids (Andrade 1983; Santos et al. 1990; Silva et al. 1970).

In order to assess the metallogenic potential of the Beja Layered Gabbroic Sequence, significant efforts were made to determine its internal architecture and related ore-forming systems. Two main styles of mineralization have been recognized previously (Jesus 2002; Jesus et al., 2003b): 1) massive Fe-Ti-V oxide accumulations within ultramafic cumulate lenses; and 2) anastomosing (locally stockwork) Cu(-Ni) sulphide vein arrays within strongly developed metasomatic halos. This paper is the first documentation of a new type of mineralization: intercummulus massive Ni-Cu-Co sulphides hosted by a pyroxenitic cumulate facies.

## 2 Geological framework

Detailed mapping of the Beja Layered Gabbroic Sequence (inset, Fig. 1) has revealed NW-trending magmatic layering that dips approximately 30°SW, typically associated with a magmatic lamination. Field and geochemical cri-

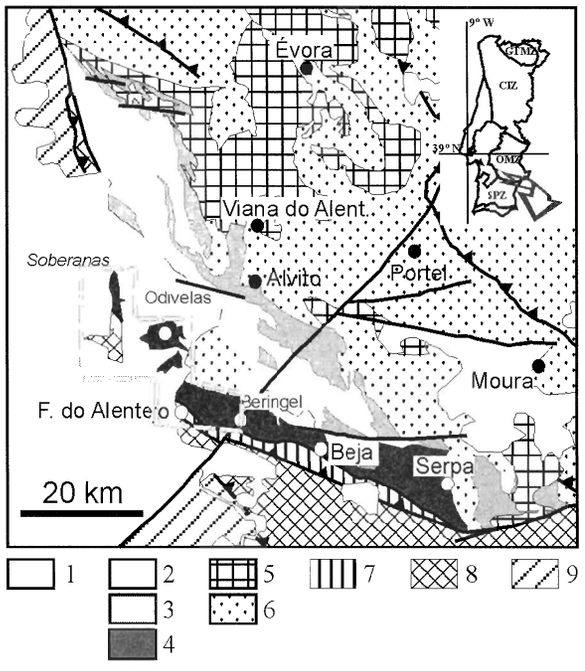


**Figure 1:** Location of the Beja Igneous Complex (BIC) with indication of the major geotectonic units of SW Iberia: CIZ, Central-Iberian Zone; GTMZ, Galicia – Trás-os-Montes Zone; OMZ, Ossa-Morena Zone; SPZ, South Portuguese Zone. Schematic geological map: 1) Cenozoic sedimentary cover; 2) Baleizão Porphyry Complex (BIC); 3) Cuba-Alvito Complex (BIC); 4) Beja Layered Gabbroic Sequence LGS (BIC). 5) Undifferentiated Variscan Granitoids. 6) Undifferentiated meta-sedimentary and meta-volcanic sequences and ultramafic rocks. 7) Beja-Acebuches Ophiolite Complex; 8) Meta-sediments and meta-volcanics of Pulo do Lobo Group. 9) Meta-sedimentary and meta-volcanic sequences of SPZ.

teria suggest that the intrusion had a multiphase history. This resulted from the input of several batches of magma, which each correspond to a distinctive series of gabbroic rocks.

Five main magmatic series were defined, from NW to SE: Soberanas I, Soberanas II, Odivelas I, II and III. The contact between Soberanas I and Soberanas II is tectonic. Soberanas I is composed of coarse-grained coronitic (leuco-) troctolite and fine grained wehrlite, whereas Soberanas II comprises fine-grained leuconorite to leucogabbro. The transition to Odivelas I is covered by Cenozoic sediments. Odivelas I consists mostly of olivine leucogabbro and includes in its lower section an intercummulus enrichment zone of vanadiferous Ti-magnetite + ilmenite, where massive type I Ti-V ores have developed (Jesus et al. 2003b). Odivelas II is a rhythmic succession of olivine gabbro with discontinuous anorthosite layers at its uppermost section. Odivelas III comprises a rhythmic sequence of well-layered olivine (leuco-)gabbro. Intercalations of fine-grained pyroxenite layers contain disseminated sulphide and sulpho-arsenide blebs, as well as anastamosing veins of pyrrhotite + chalcopyrite ± pyrite ± mackinawite, which have late-stage metasomatic haloes. These veins comprise type II mineralization (Jesus 2002; Jesus et al. 2003a). The contact between Odivelas II and III series is obscured by sedimentary cover.

Several suites of gabbroic rocks occur between Ferreira do Alentejo and Beringel. These gabbroic suites host Ni-Cu-Co- and PGE-bearing sulphide mineralization and can be correlated with Soberanas I and Odivelas II/III series. This new mineralization type occurs near Ferreira do Alentejo (Fig. 1) within a thick and rhythmic sequence of (coarse-grained) olivine leucogabbros (enclosing minor anorthosite) and pyroxenitic gabbros. Locally, these pyroxenitic gabbros grade to cumulate lenses of pyroxenite, which constitutes the preferential host of Ni-Cu-Co PGE-bearing sulphide mineralization.

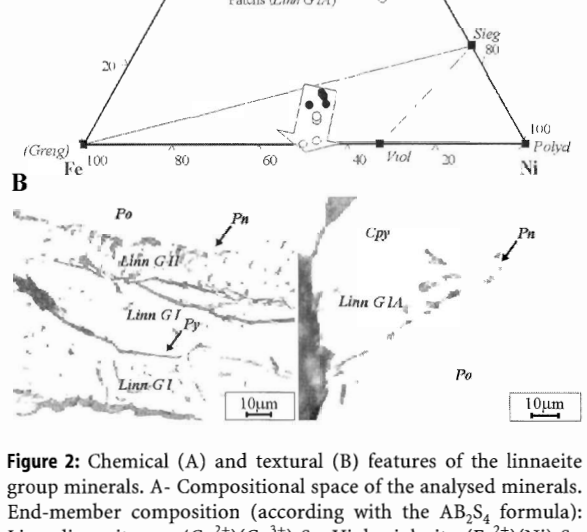


**Figure 2:** Chemical (A) and textural (B) features of the linnaeite group minerals. A- Compositional space of the analysed minerals. End-member composition (according with the $AB_2S_4$ formula): Linn, linnaeite s.s. $(Co^{2+})(Co^{3+})_2S_4$; Viol, violarite $(Fe^{2+})(Ni)_2S_4$; Sieg, siegenite $(Ni,Co)(Ni,Co)_2S_4$ (plotted empirical formula: $Ni_{2.25}Co_{0.75}S_4$); Polyd, polydymite $(Ni)(Ni)_2\ S_4$; Greig, greigite $(Fe^{2+})(Fe^{3+})_2S_4$. B- Left: typical zonation of linnaeite s.l. veins, white line indicates transition of Co-rich core (linnaeite GI) to Co-poor vein borders (linnaeite GII). Right: linnaeite s.l. GIA patches in pyrrhotite (Po) matrix bordered by pentlandite (Pn).

## 3 Ni-Cu-Co mineralization

Pyroxenites hosting the massive Ni-Cu-Co- and PGE-bearing sulphide are mainly composed of randomly oriented, subhedral grains of clinopyroxene ($En_{43}Wo_{45}Fs_{12}$). Millimetre-sized blebs of pyrrhotite with pentlandite-chalcopyrite exsolutions occur as inclusions within the coarser clinopyroxene grains, forming graphic intergrowths. As the sulphide modal proportion increases, clinopyroxene grains are disrupted, displaying abundant corrosion gulfs but only mild retrograding effects. Rare plagioclase ($An_{60}$) occurs interstitially or included within the clinopyroxene-sulphide framework. Silicate phases do not show any significant compositional zoning or retrograde textures, suggesting equilibrium with the sulphide phases. Minor magnetite ($Fe^{3+}{}_{1.59}Ti_{0.1}Cr_{0.1}V_{0.03}Al_{0.07}\ Fe^{2+}{}_{1.08}\ Mg_{0.04}Mn_{0.01}O_4$) and ilmenite ($Fe^{2+}{}_{0.84}Mg_{0.06}\ Mn_{0.06}Fe^{3+}{}_{0.05}V_{0.05}\ Ti_{0.95}O_3$) coexist with pentlandite-pyrrhotite-chalcopyrite blebs suggesting $fO_2$ conditions of late stage (~620 °C) crystallization close to QFM.

Groundmass and disseminated pyrrhotite blebs display similar Fe:S (0.87) and Ni contents (0.01 (atoms per unit formula) suggesting that the massive ores developed by coalescence of monosulphide droplets as sulphide saturation was achieved. pentlandite exsolutions have an almost invariant (Co+Ni):Fe ratio of 1.2-1.4 and an average formula $Fe_4Ni_{4.3}Co_{0.6}S_8$. Linnaeite group minerals (*linnaeite s.l.*) have sealed a network of intra- and intergranular millimetric veinlets that crisscross the pyrrhotite matrix. Electron microprobe data confirms that these veins have complex compositional zoning that results from multiphase infilling, as indicated by petrographic observations (Fig. 2).

Early *linnaeite s.l.* Co-rich vein cores are rimmed by a dissymmetric (sometimes absent) Co-poor border, whereas irregular patches with intermediate Co contents are observed in the pyrrhotite matrix; pentlandite occurs on the edges of these patches (Fig. 2B). Ideal metal site distribution according with the (thio-) spinel-like structure of linnaeite group minerals shows that the analysed minerals are non-stoichiometric: *linnaeite s.l.* Co-rich vein cores $(Fe)_1(Fe_{0.3}Ni_{1.5}Co_{0.4})_{\Sigma 2.2}\ S_{3.9}$; *linnaeite s.l.* Co-poor vein borders $(Fe)_1(Fe0_{.5}Ni_{1.5})_{\Sigma 2}S_4$ and *linnaeite s.l.* patches in pyrrhotite matrix $(Fe)_1(Fe_{0.3}Ni_{1.5}Co_{0.2})_{\Sigma 2}\ S_4$. The resulting deviation is due to exceeding Fe in the B position, displacing the trend towards a greigite composition

**Table 1:** EPMA trace element average contents (ppm) of the sulphide phases (maximum and minimum in parenthesis) normalized for 100 wt%. N = number of analyses; nd= below detection limit. Py VL = pyrite late veinlets occurring in the core of linnaeite s.l. zoned veins; Py G = early pyrite grains in the pyrrhotite matrix; Py VG = pyrite veins in pyrrhotite matrix; Ccp = chalcopyrite exsolutions in pentlandite blebs; Po = pyrrhotite blebs and groundmass; Pn = pentlandite exsolutions in pyrrhotite blebs; Linn GI = linnaeite s.l. Co-rich vein cores; Linn GII = linnaeite s.l. Co-poor vein borders; Linn GIA = linnaeite s.l. patches in pyrrhotite matrix.

| | Pd | Ag | Cd | Pt | Au | Bi | N |
|---|---|---|---|---|---|---|---|
| *Py VL* | 26 (51-1) | 268 (535-1) | 479 (956-1) | *nd* | 275 (550-1) | 262 (522-1) | *2* |
| *Py G* | *nd* | 137 (273-1) | 56 (110-1) | 48 (94-1) | *nd* | *nd* | *2* |
| *Py VG* | 183 (537-1) | 65 (160-1) | 386 (1308-1) | 271 (874-1) | 19 (89-1) | 196 (790-1) | *5* |
| *Ccp* | 879 (1034-723) | 334 (667-1) | 646 (1291-1) | *nd* | 346 (692-1) | 427 (698-156) | *2* |
| *Po* | 298 (708-1) | 172 (925-1) | 570 (1075-1) | 133 (593-1) | 126 (751-1) | 284 (1244-1) | *6* |
| *Pn* | *nd* | 694 (1116-459) | 382 (1447-1) | 497 (1235-2) | 360 (1768-1) | 289 (958-1) | *6* |
| *Linn GI* | 197 (784-1) | 40 (158-1) | 253 (732-1) | 535 (1614-2) | 206 (822-1) | 112 (327-1) | *4* |
| *Linn GII* | 295 (588-1) | 213 (425-1) | 27 (53-1) | *nd* | *nd* | 136 (234-39) | *2* |
| *Linn GIA* | 405 (810-1) | 699 (1078-320) | 196 (391-1) | 155 (308-2) | *nd* | *nd* | *2* |

(Fig. 2A). The *linnaeite s.l.* Co-rich vein cores present the maximum deviation accompanied by sulphur deficiency, a common feature in non-stoichiometric minerals of the linnaeite group. Late veinlets of Ni-rich pyrite in the *linnaeite s.l.* zoned veins ($Fe_{0.9}Ni_{0.1}S_2$) include trace amounts of Co (726-1147ppm). Millimetric veinlets of pyrite in the groundmass and occurring as early-formed subhedral grains display gradually lower Ni contents from 11666 to 7300 ppm. Late-stage chalcopyrite occurs in microfractures and has locally replaced earlier-formed sulphides.

Semi-quantitative EPMA data for trace elements in sulphide phases are shown in Table 1. Higher Pt, Ag and Au contents were measured consistently from the rims of pentlandite, suggesting that cryptic mineral exsolutions incorporating those metals may be present. Chalcopyrite has the highest analysed Pd concentration (1034 ppm). Pd/(Pt+Au) is strongly partitioned between chalcopyrite and pentlandite with (Pt+Au) displaying higher affinity with the Co-Ni-rich phase. All *linnaeite s.l* phases display negative correlation between Co contents and Pd/(Pt+Au) ratio. Thus, *linnaeite s.l* compositional (Co) variations may represent a suitable pathfinder for high (Pt+Au) grades.

## 4 Conclusions and future research

The results of this study demonstrate the occurrence of primary magmatic Ni-Cu-Co and PGE-bearing sulphide mineralizations in the Beja Layered Gabbroic Sequence, providing new insights into the metallogenic potential of this igneous complex. Further research is underway to fully explore the economic significance of these new findings.

## Acknowledgements

The authors acknowledge the financial support of CREMINER and Centro de Geologia-FCUL. Part of this work was supported by the research project 12/2.1/CTA/82/94– PROGEREMIN. Ana Jesus acknowledges a PhD Grant SFRH/BD/6355/2001. D. Cooke is gratefully acknowledged for is reviews of this paper.

## References

Andrade AS (1983) Contribuition à l'analyse de la suture Hercynièn ne de Beja (Portugal), perspectives metallogéniques. Ph.D. thesis, INLP, Univ. of Nancy, France (English abstract)

Dallmeyer RD, Fonseca PE, Quesada C, Ribeiro A (1993) $^{40}Ar/^{39}Ar$ mineral age constraints to the tectonothermal evolution of the Variscan Suture in SW Iberian. Tectonophysics 222: 177-194

Jesus AP (2002) Fe-Ti-V mineralizations and sulphide occurrences in gabbroic rocks of the Beja Igneous Complex (Odivelas–Ferreira do Alentejo). M.Sc. thesis, University of Lisbon (English abstract)

Jesus AP, Mateus A, Oliveira, V Munhá J (2003a) Ore forming systems in the Layered Gabbroic Sequence of the Beja Igneous Complex (Ossa Morena Zone, Portugal); state of the art and future perspectives. In: Eliopoulos, DG et al. (eds), Mineral Exploration and Sustainable Development. Proceedings Volume of the 7th Biennial SGA Meeting, Athens, Greece, August 24 - 28, 2003. Milpress, Rotterdam Netherlands: 591-594

Jesus AP, Mateus A, Waerenborgh JC, Figueiras J, Cerqueira L, Oliveira V (2003b) Hypogene titanian, vanadian maghemite in reworked oxide cumulates in the Beja Layered Gabbro Complex, Odivelas, Southeastern Portugal. Canadian Mineralogist 41: 1105-1124

Santos JF, Andrade SA, Munhá J (1990) Orogenic magmatism in the meridional border of the Ossa Morena Zone. Comunicações Serviços Geológicos de Portugal 76: 91-124 (English abstract)

Silva LC, Quadrado R, Ribeiro L (1970) Preliminary notes about the existence of a zoned structure and of anorthosites in the gabbro-dioritic massif of Beja. Boletim Museu Laboratório Mineiro Geológico da Universidade de Lisboa 11: 223-232 (English abstract)